3D Reference Trajectory Optimization Using Particle Swarm Optimization

Conference Paper · June 2017

DOI: 10.2514/6.2017-3435

4 authors, including:

Alejandro Murrieta Mendoza
Amsterdam University of Applied Sciences/Centre for Applied Research on Education

Hugo Ruiz
Laboratoire d'Informatique, de Robotique et de Microélectronique de Montpellier (LI…

Ruxandra Mihaela Botez
École de Technologie Supérieure

3D Reference Trajectory Optimization Using Particle Swarm Optimization

Alejandro Murrieta-Mendoza[1], Hugo Ruiz[2], Sonya Kessaci[3], Ruxandra Mihaela Botez[4]
Université du Québec, École de Technologie Supérieure
Laboratory of Research in Active Control, Avionics, and Aeroservoelasticity LARCASE
Montreal, Quebec, H3C 1K3, Canada

Reference trajectory optimization is a way to reduce fuel burn, thus reducing the polluting emissions released to the atmosphere. In this paper, the Particle Swarm Optimization was implemented to find the most economical 3D reference trajectory in terms of fuel burn and flight time. The aircraft fuel burn was obtained using a numerical model created from experimental flight data. The algorithm is able to follow Air Traffic Control constraints such as constant altitude segments, changes of altitudes and fixed Mach number. The free flight concept was implemented as the aircraft can fly anywhere in the search space. Results showed that the algorithm was able to generate realistic trajectories as changes of altitudes were not executed at consecutive waypoints, and changes of aircraft`s direction were executed following long segments of constant direction. Trajectories converge towards the optimal trajectory. The algorithm showed that it has the potential to provide savings of up to 6.48% in terms of fuel burn.

Nomenclature

B_l	Best local trajectory position
B_g	Best global trajectory position
c_1	Influences the particle's movement in relation with the best local optimal
c_2	Influences the particle's movement in relation with the global optimal
D	Particle's displacement
i	A trajectory
j	Dimension to mutate: Lateral or vertical.
k	Current iteration
R_1	Random value affecting the influence of local optimal
R_2	Random value affecting the influence of global optimal
R_ω	Random value affecting the influence of the particle's inertia
ω	Particle Inertia
X	Particle's next location

I. Introduction

REFERENCE trajectory optimization, (The trajectory that the aircraft should follow to fly from airport A to airport B in terms of ground track, speeds and altitudes) is an interesting way to reduce the fuel consumption, hence it is helpful to reduce the polluting emissions released to the atmosphere and to reduce the flight cost. Pollution is of great concern for the aeronautical industry due to global warming and future taxation to emissions proposed by different organisms and states. Carbon Dioxide (CO_2) is of special interest due to its known effects in global warming. This can be seen in a recent study where for a city pair transatlantic flight, the total flight time, thus the fuel burn, required to perform this type of flights has increased due to the CO_2 effect in wind patterns [1]. Different

[1] Ph.D Student, Université du Québec LARCASE, 1100 Notre Dame, Montreal, QC, H3C 1K3, Canada.
[2] Undergraduate Student, Université du Québec, LARCASE, 1100 Notre-Dame, Montreal, QC, H3C 1K3, Canada.
[3] Undergraduate Student, Université du Québec, LARCASE, 1100 Notre-Dame, Montreal, QC, H3C 1K3, Canada.
[4] Professor, Université du Québec, LARCASE, 1100 Notre-Dame, Montreal, QC, H3C 1K3, Canada.

reports have shown that around 2% of the total CO_2 released to the atmosphere due to human activity are attributed to aeronautical activities [2]. Among other components released to the atmosphere due to fuel burn we can find Nitrogen Oxides (NOx) and hydrocarbons. An analysis

There exists technologies to reduce fuel burn such as winglets [3], morphing wings [4], state of the art aerodynamics, and etcetera. However, these technologies require important structural modifications demanding high investment by the aircraft operator. Winglets require reconstructing the wingtips, morphing wings for commercial aircraft a technology that will require important wing modifications has not reached its full maturity. State of the art aerodynamics are taken into account for every new generation of aircraft. However, developing and certifying a new aircraft is a long and complicated task. Besides, only replacing current aircraft for the latest models wouldn't be enough to meet the carbon reduction goals[5]. Additional measures are required.

Relatively simple measures taken by the operator such as washing engines before take-off, reduce the aircraft weight, assisted or one engine taxi, and etcetera also contribute to reducing fuel burn[6] .There has also been different research aiming to reduce fuel consumption by optimizing different operations such as taxiing and developing assisting decision tools[7].

Reference trajectory optimization on the other hand could be simple to implement in ground systems or it can be contained in avionics devices such as the Flight Management System (FMS).

Although the importance of trajectory optimization to reduce pollution is well known within the aeronautical industry, different studies have shown that aircraft do not fly at their optimal speeds and altitudes [8, 9]. This can be attributed to different causes such as the airspace being too crowded, inefficiency of air traffic management, a lack of tools available to the dispatcher, important changes between the wind forecast and the actual wind encountered by the aircraft, or by airline policies requiring faster inefficient flights [10].

Research has been conducted by different groups in order to develop algorithms able to optimize the aircraft reference trajectory. Lidén[11] studied the influence of winds in selecting the places where to execute the step climb, and four different filtering methods were proposed to achieve an operational commercial flight trajectory in a FMS.

An algorithm able to determine the optimal constant cruise altitude was developed[12]. Dynamic programming was implemented[13] to solve the combination of speeds and altitudes that provide the most economical cost for a 3D trajectory (ground track, speed and altitude) for the complete vertical reference trajectory (climb, cruise, and descent). Golden Section Search was as well proposed [14] to find the most economical altitudes to perform a short flight. Beam search, a variation of branch and bound, was presented in order to solve the vertical reference trajectory for short and long flights [15]. This method was then improved where the Beam search was executed after a space search reduction causing the algorithm to converge faster to the optimal solution[16]. Optimal control was as well implemented to find the optimal vertical reference trajectory for the cruise phase only respecting current air traffic management [17].

Algorithms modifying the ground track at constant altitude aiming to take advantage of winds to reduce the required fuel burn to flight a given trajectory have also been developed. Such is the case of the Dijsktra's algorithm which was used to avoid objects for general aircraft [18]. Dijkstra's algorithm was also used to optimize the trajectory for a commercial airliner[19].

Optimizing the lateral and the vertical reference trajectory normally provide more fuel burn reductions. This was studied[20] where the most economical lateral reference trajectory was computed, then the waypoints location where to execute step climbs were identified. A*, a variation of Dijkstra's algorithm, was implemented [21] to simultaneously optimize the 3D reference trajectory while avoiding objects. Genetic algorithms were used to simultaneously compute the waypoints' location that provided the most economical flight cost [22].

Contrails, clouds formation due to aircraft activity, are believed to cause even more harm than CO_2. Trajectory optimization algorithms avoiding zones where the weather conditions are favourable to generate contrails were avoided, and a cost was attributed when the aircraft had to fly within those contrail-formation zones [23, 24].

Dynamic programming coupled with neuronal network were implemented[25] for a 4D reference trajectory (ground track, altitude, speed, and time constraint). Dynamic programming was also used with a new iterative variation[26].

The algorithms proposed above, except genetic algorithms, are of deterministic nature (they always provide the same solution and its decision process is well structured making them easy to track). Another alternative is using metaheuristic algorithms as they can explore a greater search space for solutions. However, these algorithms are *unpredictable* because they normally use a random behaviour to diversify its search. Metaheuristic algorithms do not guarantee providing the global optimal, nevertheless, they tend to provide solutions close to the optimal trajectory in a fraction of the time required by deterministic algorithms.

Among the metaheuristic algorithms studied in the literature, we can find genetic algorithms, Artificial Bees Colony (ABC), and Artificial Colony Optimization (ACO). Besides the 3D as presented before, Genetic algorithms were also used to find the most economical trajectory in the flight trajectory in 4D [27]. The Artificial Bees Colony (ABC) was implemented in 4D achieving interesting results in optimization and fulfilling the required time of arrival constraint [28]. Artificial Colony Optimization (ACO) was implemented [29, 30] to optimize the lateral reference trajectory and to find the most economical combinations of Mach numbers that fulfill the RTA constraint.

It is known that Particle Swarm Optimization (PSO) provides good results to combinatory problems such as the reference trajectory optimization problem. However, in spite the number of algorithms used to find the most economical trajectory, the PSO has not been explored to optimize the reference trajectory for commercial aircraft. As ABC and ACO are based on the PSO and have provided good results, it is of interest to study this algorithm. The objective of this paper is to develop an optimization algorithm that simultaneously optimizes the reference trajectory optimization in 3D (vertical and lateral reference trajectories). Weather and traffic management constraints such as constant altitude segments and constant Mach number were taken into account.

This paper is organized as follows. First the aircraft and the weather models are presented. Secondly the flight cost methodology is described, thirdly the PSO algorithm is explain, and then the implementation for the reference trajectory problem is described. Finally results and conclusions are presented.

II. Aircraft Fuel Burn and Search Space, and Weather Forecast Models

A. The Numerical Performance Model

The aircraft fuel burn model is provided under the form of a discrete numerical performance model developed from experimental flight test data. This model provides the fuel flow a constant altitude and a constant Mach number flight. This model also provides the fuel burn, and the horizontal traveled distance required to climb (or descent) from a given altitude to a target altitude. This model is seen as a black box where all inputs should be available to obtain the required output. This model is described in Table 1 where *ISA Dev Temperature* refers to the International Standard Atmosphere (ISA) temperature deviation.

Table 1. The Numerical Performance Model Inputs/Ouputs for Different Flight Phases

Flight Phase	**Inputs**	**Outputs**
Cruise	Grossweight (kg) Altitude (ft) ISA Dev Temperature(C) Mach Number	Fuel Flow (kg/hr)
Climb	Grossweight (kg) Altitude (ft) ISA Dev Temperature (C) Mach Number	Fuel Burn (kg) Horizontal traveled distance (nm)
Descent	Grossweight (kg) Altitude (ft) ISA Dev Temperature (C) Mach Number	Fuel Burn (kg) Horizontal traveled distance (nm)

The *Cruise* phase refers as the aircraft being flying at constant altitude and constant Mach number. The *Climb* phase refers to the aircraft performing a step climb during cruise at constant Mach number, and *Descent* phase refers to the aircraft executing a step descent during cruise at constant Mach number.

B. The Weather Forecast Model.

Weather is very important in aviation as it has a strong effect in flight cost. Temperature affects the engine's performance thus the required fuel to produce the required thrust. Headwinds and tailwinds modify the ground speed, thus changing the flight time: headwinds *forces the aircraft* back, extending the flight time and therefore, make the flight longer (more fuel). On the contrary, the tailwinds *exert force* on the aircraft, reducing the flight time (less fuel).

The weather forecast used in this algorithm was taken from Weather Canada. This forecast consists in a 0.6 km x 0.6 km grid divided in 3 hours block (from 0h to 144h) and at different pressures (altitudes). At each point of the grid, different information is available, such as temperature, wind speed and wind direction.

As aircraft is rarely located on the exact position of the forecast grid, it is necessary to make interpolations in time, flight level and position to find the required weather. Fig. 1 describes the interpolations orders for weather. First, interpolations are executed in time, then in flight level, and finally bilinear interpolations for the weather.

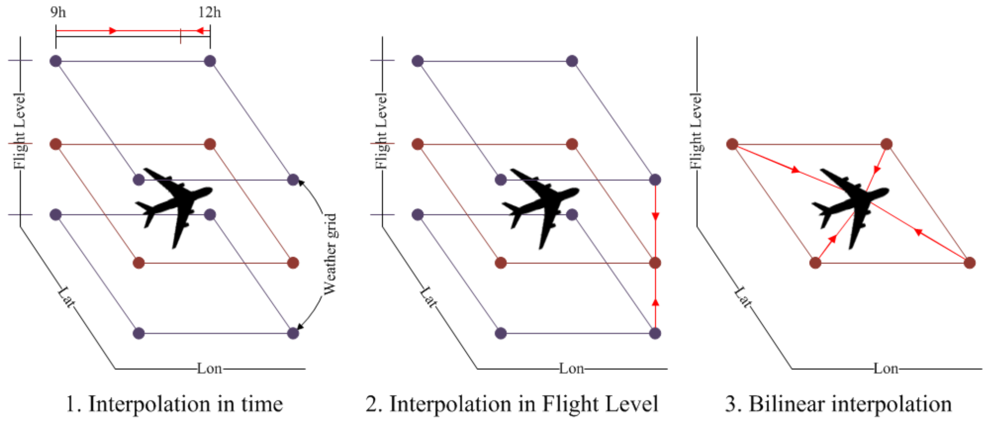

Fig. 1 Interpolations to have weather information at the exact aircraft's coordinate

Weather information is used to compute two parameters: Ground Speed, and ISA temperature deviation as in Eq. (1) and Eq. (2)

$$GS = TAS \pm WS \cos(\varphi - WD) \tag{1}$$

where *TAS* is the True air Speed, *WS* is the wind speed, *WD* is the wind angle and φ is the aircraft's azimuth.

$$ISA\ DEV\ Temperature = Temp(Alt) - ISA\ Temp\ (Alt) \tag{2}$$

where *Temp* is the temperature obtained from the weather forecast at the current cruise altitude, and *ISA Temp* is the expected temperature according with the ISA atmosphere.

C. The Fuel Burn Computation

The aircraft's weight changes during flight due to the fuel burned. Consequently, the aircraft's weight is not always the exact pre-set value defined in the numerical performance model. The *ISA_DEV* parameter presents the same behaviour of not being the exact value available in the numerical performance model as temperature changes along the flight. For these reasons interpolations to compute the required parameters are performed for the weight and temperature.

The reference trajectory is divided in segments defined by the number of waypoints in the trajectory of reference. After that, each segment is divided in 20 nautical mile sub-segments to have enough accuracy in the flight cost computation with a low computation time. At each sub-segment, the next operations are performed.

1. The fuel burn required to fly the previously segment is removed from the aircraft's gross weight.
2. With weather information (temperature, wind direction and wind speed), the Ground Speed (GS) and the ISA_DEV can be computed.
3. Linear interpolations are performed to calculate the fuel flow, the fuel burn or the horizontal traveled distance for the current sub segment.

For the analyzed flight, there exist two different cases in which the fuel burn is computed: when the aircraft is in cruise (constant altitude) and when it is required to climb or descend during cruise (different altitudes)

<u>Constant Altitude</u>

As it is shown in Table 1, the numerical performance model provides fuel burn for this phase as *Fuel Flow* (kg/hr). For this reason, the *Flight Time* required to compute the *Fuel Burn* for a given segment is computed using the *GS* computed as in Eq (1). The fuel burn can be computed with Eq (3).

$$Fuel\ Burn(kg) = Fuel\ Flow\left(\frac{kg}{hr}\right) \times Flight\ Time(hr) \tag{3}$$

Variation of altitude

When, for the given segment, there is a change of altitude; the data provided from the numerical performance model allows computing the fuel burn, and the horizontal traveled distance to climb from the initial altitude to the objective altitude. Once the objective altitude has been attained, the rest of the fuel burn for the segment is computed as a fixed altitude. The process to compute the fuel burn for a segment where a change of altitude is required, the next steps are followed

1. The fuel burn required to fly the previously segment is removed from the aircraft's gross weight.
2. The fuel burn and the required horizontal distance required to change altitude (climb or descent) are computed.
3. The fuel burn computed to change altitude is subtracted from the aircraft's gross weight.
4. The required horizontal distance is subtracted from the segment distance (e.g, New Segment Distance = 20 nm – *horizontal traveled distance*).
5. The rest of the segment is computed as a constant altitude using the new segment distance.

D. Search space

An aircraft under *free flight* can go anywhere in the airspace. This brings an infinity of possibilities to create a trajectory. Finding the optimal trajectory is a complex problem to be solved. For this reason, the search space is modeled under the form of a unidirectional graph G (V,E) where V are the nodes where the aircraft can fly to, and E are the links between every node. For the algorithm, every node is connected to its consecutive neighbours.

1. Search Space for the Vertical Reference Trajectory

The search space for the vertical reference trajectory consists in the nodes defined per altitude. Commercial long haul aircraft normally fly the cruise phase at altitudes from around 26,000 ft to 41,000 ft. These limits are defined as boundaries.

Vertical Reference Trajectory Boundaries

The boundaries for the vertical reference trajectory are defined in altitude and in flying distance.

- The flight distance defined is the distance between the ToC and the ToD.
- The minimal and the maximal cruise altitude.

The vertical reference trajectory search space is shown in Fig. 2.

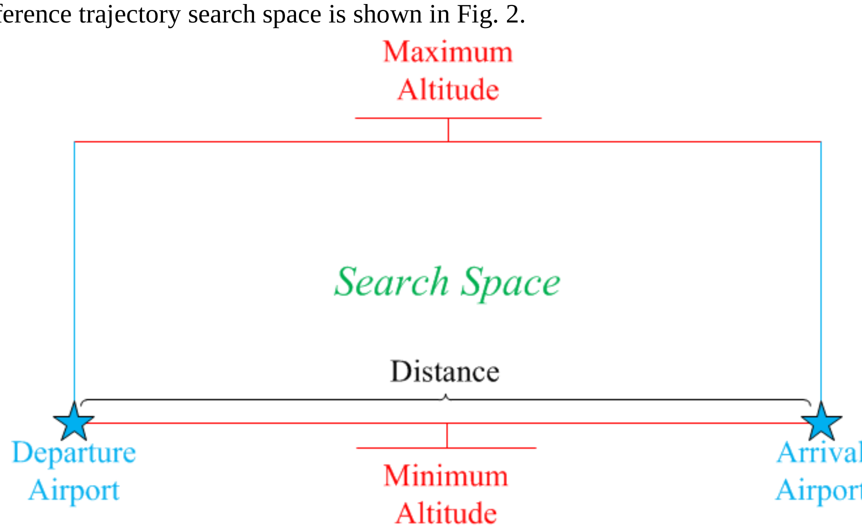

Fig. 2 Search space for the vertical navigation

The ground track waypoint placement

The change of altitude is only allowed when the aircraft is at a node. For this reason, the number of nodes selected to create the graph is important and has an impact on the algorithm performance. By putting a large number of nodes, trajectories have a better resolution. However, there would be more combinations which would increase the computation time. As a concession between a precise search space and a short computation time, 34 waypoints were selected as the ground track nodes for a long haul flight. Flights normally fly at altitudes multiple of 1,000 ft. In the first instance, the search space is separated in1,000 ft. This gives a result a graph such as the one in Fig. 3.

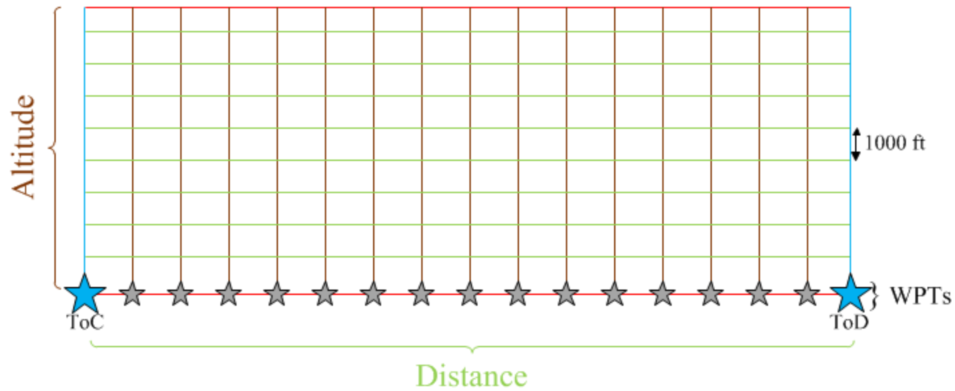

Fig. 3 Search space with 34 waypoints, made for the cruise phase

Due to air traffic restriction, flights with a westbound direction fly at odd altitudes and flights with an eastbound direction fly at even altitudes [31]. Therefore, when the aircraft requires a change of altitude, step climbs of 2000 ft are executed. As a consequence, the aircraft can reach the ToD at any altitude within the imposed boundaries. The final search space taking into account the step climb restrictions is shown in Fig. 4.

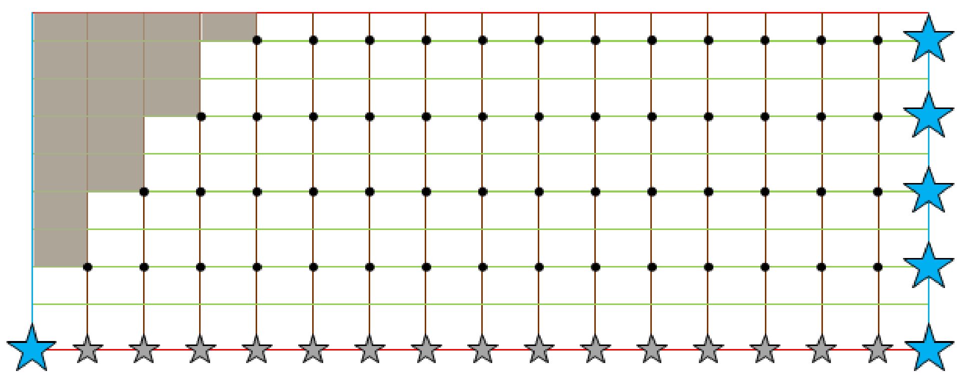

Fig. 4 Search space with the entire 2000ft step climb

2. *Search Space for the Lateral Reference Trajectory*

The search space for the lateral reference trajectory consists in the changes of direction an aircraft can execute during a flight. For this, a trajectory of reference is selected. It could be any trajectory, for example the great circle (geodesic) between the departure and arrival airport (blue stars on Fig 5), a pre-computed trajectory or a trajectory from an historical flight. Nodes with displacements of around 7.5 to 15 degrees are placed in front of a given node. The graph created around the trajectory of reference (grey) is on Fig 5.

Fig 5 Search space for the lateral reference trajectory created around a geodesic reference trajectory

Lateral Reference Trajectory Boundaries

There are two different boundaries to define the search space.

- The first boundary is the flight distance defined by the ToC and the ToD.
- The number of *corridor* of the lateral trajectory. For example, there are 5 corridors: the reference trajectory, two above it, and two below it.

Fig. 6 Search space for the lateral navigation with the boundaries

3D Search Space

For the 3D reference trajectory space, the lateral and the vertical search spaces are blended together to create the 3D search space.

III. Methodology

A. The PSO Generalities

The Particle Swarm Optimization (PSO) algorithm reproduces the social behaviour of animals such as fish school or the displacement of bird flock. The operating of this algorithm is different than other social algorithms, the particularity of the PSO algorithm it's that they have leader contrary to ant colony or bee colony which are based on intelligence of a group. The PSO optimizes following a leader, this leader can be replaced if another particle is better. In nature this can be seen as the bird flock leader rotates as the leader gets tired.

The original PSO algorithm progresses by iterations. At every single iteration, each particle searches a solution within the search space. This search is performed by a particle's movement influenced by three different parameters: the position of the global best trajectory for all particles, the position of best local trajectory (not for all particles but for a group of particles) and the displacement inertia. The mains equations in the PSO are Eq. (4) and Eq. (5).

$$D_i\{j\}(k+1) = \omega R_\omega D_i\{j\}(k) + c_1 R_1\big(B_l\{j\} - X_i\{j\}(k)\big) + c_2 R_2\big(B_g\{j\} - X_i\{j\}(k)\big) \quad (4)$$

$$X_i\{j\}(k+1) = X_i\{j\}(k) + D_i\{j\}(k+1) \quad (5)$$

where *i* is a trajectory, k is the current iteration. *D* represents the particle's displacement associate with the parameter *j*, which indicates if the displacement is in the lateral or vertical reference trajectory. *X* is the next particle's location. B_g refers to the best global trajectory position, B_l refers to the best local trajectory position. In order to have an influence in convergence, there are 3 random parameters R_ω, R_1 and R_2 with values between 0 and 1. The role of these parameters *R* is to determine the, B_g, B_l and the influence on the particle's movement. The parameters c_1 and c_2 are positive constants provided by the user which influences the particle movement in reference to the B_g, B_l trajectories. The parameter ω refers to the aircraft's inertia and it is set by user. The inertia represents the particles tendency to keep the same direction.

B. General Operating of the PSO algorithm

The algorithm operates by blocks as shown in **Error! Reference source not found.**. The first step is the input of all parameters such as number of waypoints, size of the graph, latitude, longitudes, altitudes, and etcetera. After this step, there is the creation of all the initial random trajectories; this part will be explained more in detail in the next Section. Once all the initial trajectories were created, the algorithm makes a first selection of trajectories before beginning the PSO in order to define the best global and the best local trajectories. After the PSO has been executed, the most economical trajectory found by the algorithm is returned to the user
.

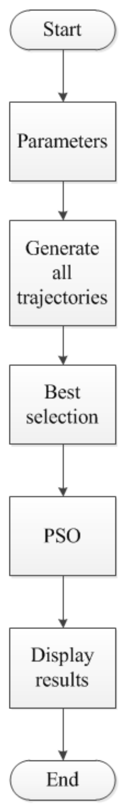

Fig. 7 General Operating

C. The PSO and the 3D Reference Trajectory Optimization

In the developed algorithm, *D* and *X* correspond to the set of altitudes or latitudes per each waypoint. For a given vector *WPT* containing the waypoints of reference, the vectors *D* and *X* map the altitude and the latitude position of each waypoint to the corresponding WPT. For example, for vector *WPT* containing *n* reference waypoints of a given flight as in Eq (6), there are a vector *D* and a vector *X* with *n* elements as in Eqs. (7) and (8).

$$WPT_i = [wpt_i^1, wpt_i^2, \dots, wpt_i^n] \tag{6}$$

$$D_i = [d_i^1, d_i^2, \dots, d_i^n] \tag{7}$$

$$X_i = [x_i^1, x_i^2, \dots, x_i^n] \tag{8}$$

For each waypoint, the algorithm computes a displacement *D* according to the global best trajectory B_g which is the most economical trajectory and the local best trajectories B_l the current best economical trajectory among a group of trajectories. For n waypoints and the trajectory number i, the displacement will be having the form following:

There could be cases when the displacements *D* bring as a result positions *X* outside the boundaries or outside a pre –defined s maximum value. In these cases, the algorithm corrects the vector *X* for any discrepancy.

1. Operating of PSO function

In **Error! Reference source not found.**, the drawing shows step by step the operating of the algorithm to make the Particle Swarm Optimization.

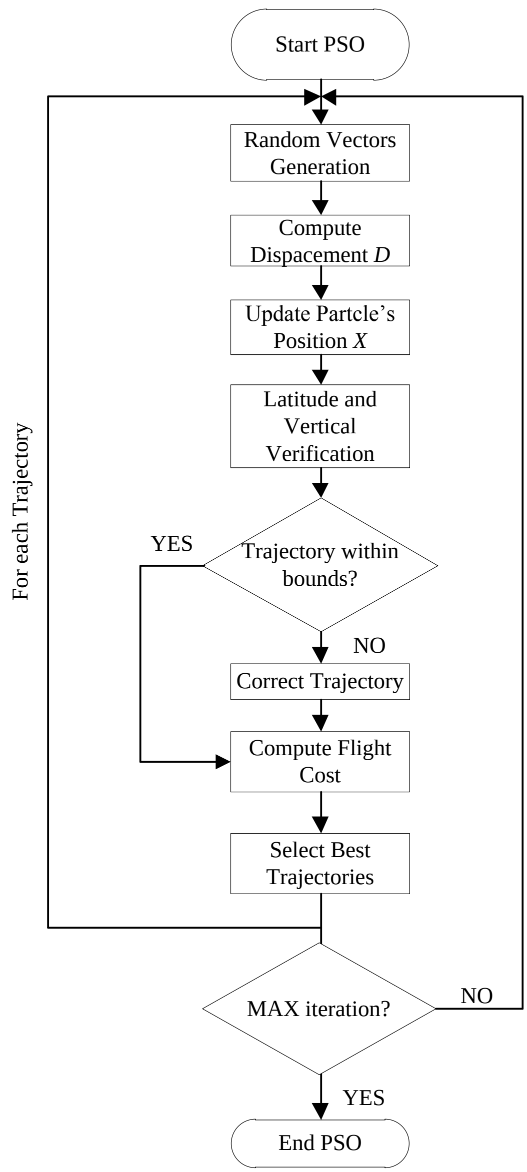

Fig. 8 General operating of the PSO

In a first phase, the random vectors R_ω, R_1 and R_2 in Eq (**4**) necessary to the algorithm are created. The displacement is then computed, and the trajectories are update. It is then necessary to verify that all the new geographical coordinates and altitudes are within the boundaries (This is explained below). Two cases appear: the position X is within bounds, and, on the contrary, the position X is out of bounds. If the position X is within limits, the algorithm can continue to the next step, otherwise it corrects any discrepancy. After these steps, the trajectory cost is computed. The selection of the global best and the local is possible. This process is repeated for each trajectory.

2. Vertical verification

The random values in Eq (8) gives as a result positions X that are rarely exactly at a 1,000 ft pair. For example, the vector X for altitude can be as in Eq (9).

$$\begin{pmatrix} 34000 \\ 34000 \\ 35792.2 \\ 35185.6 \\ 36201.1 \end{pmatrix} \rightarrow \begin{pmatrix} 34000 \\ 34000 \\ 36000 \\ 36000 \\ 36000 \end{pmatrix} \tag{9}$$

In Eq. (9), there are waypoints with an altitude such as 35792.2. The algorithm identifies these altitudes and corrects them to their closest value available within the graph.

After this correction, the trajectory may present some disparities that make the trajectory to be difficult to be followed in practice. The algorithm tries to identify and to correct such disparities. Fig. 9 shows the 4 disparities considered in the algorithm for the vertical reference trajectory:

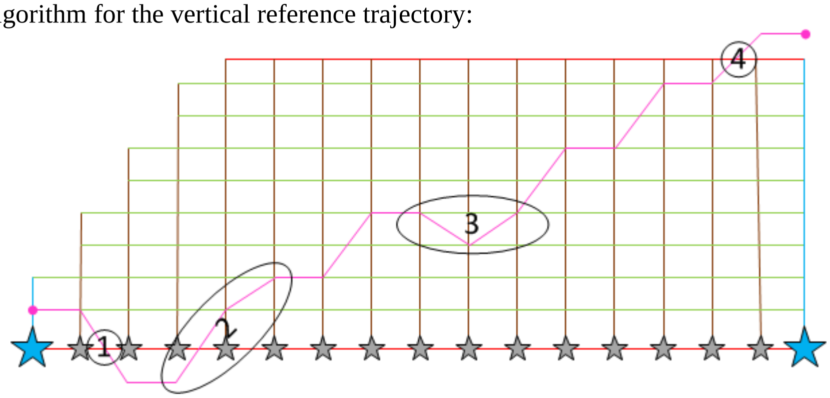

Fig. 9 Disparities on an example trajectory after the displacement

For the first disparity, the trajectory tries to descent outside the boundary limits; in this case, the algorithm will fix the waypoints at the minimum altitude in order to stay in the limits.

The second disparity corresponds at two consecutive step climbs, under normal circumstances the aircraft stays for a while at fixed altitude after a change of altitude. Moreover, the step climb which the aircraft try to execute are only of 1000 ft. Thus, the aircraft stays at the same altitude.

The third disparity is similar than the second one. The aircraft descents and at the next waypoint it climbs to reach the same altitude. This may be absurd and it would also require ATM authorization. The aircraft is set to keep the same altitude.

Finally, at the fourth disparity, the aircraft try to reach an altitude higher than the maximum altitude, the algorithm defines the puts the value of the limit to altitude at the waypoint.

After fixing all this disparities, the *fixed* trajectory is shown in Fig. 10:

Fig. 10 Vertical Reference Trajectory After correcting the Trajectory Displacement Errors

3. Lateral verification

First, the possible latitudes for the current waypoint (the latitude defined during the search space), from the graph are recovered under the form of a vector in order to determine if they are close to the computed *X* latitude.

If there are exactly the same, the waypoints keep this new latitude. On the other hand, if the new and the pre-defined latitude are different, the new latitude takes the closest value found in the search space. This can be seen in Fig. 11.

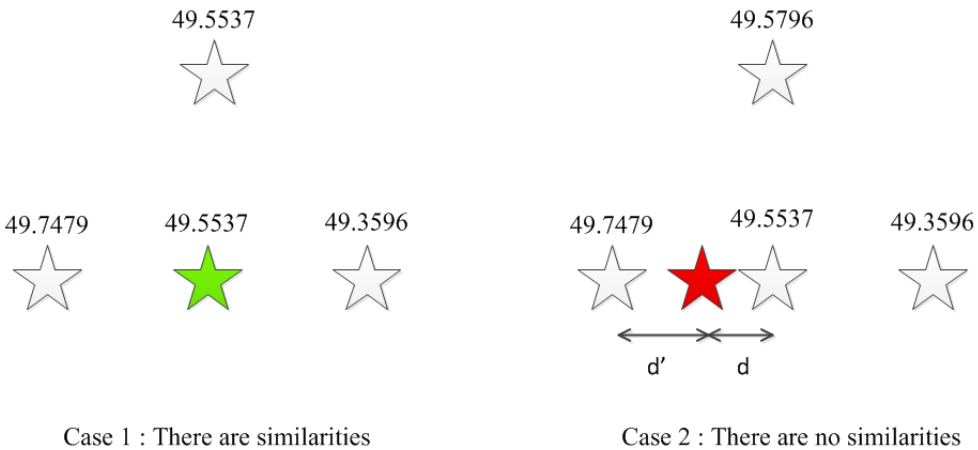

Fig.11 Different cases for the lateral verification

During the lateral reference trajectory, the aircraft can only go from the current waypoint to the next consecutive straight waypoint, or the next consecutive waypoints at the left or at the right as shown in Fig. 12:

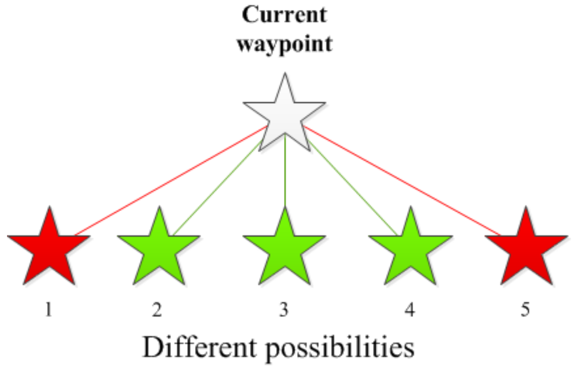

Fig. 12 Possible waypoint selection while creating the lateral reference trajectory.

Once a trajectory is created, the algorithm verifies its validity and fixes any discrepancy. The 3 cases taken into account are shown in Fig. 13

Fig. 13 Lateral Reference Trajectory With Waypoint Selection Discrepancies

The first discrepancy consists in a waypoint selection that is not one of the three closest consecutive waypoints. The waypoint is located to the closest valid waypoint.

In the second discrepancy, it can be seen that the resulting waypoint is out of the graph surpassing the boundaries. The waypoint is placed at the limit.

The last discrepancy corresponds to the fact that the algorithm is trying to reach a non-existing waypoint. The algorithm places the waypoint to the closest available one.

After fixing all these discrepancies, the valid trajectory takes the form such as in Fig. 14

Fig. 14 New lateral trajectory

After a change in latitude, many parameters such as longitude, azimuth and the distance between 2 waypoints are recomputed.

IV. Results

Different tests were performed in order to show some the capacity of the Particle Swarm Optimization in optimizing aircraft reference trajectories.

The first set of testd has been executed for the long haul flight Montreal (YUL)-Paris (CDG), with a time of take off at 10AM. As for coefficients ω = 0.73 c_1 = 1.50 and c_2 = 1.50. The goal of this tests is to observe the algorithm convergence for the the lateral and the vertical reference trajectory which composed the 3D search space.

1. Algorithm Convergence

<u>*Vertical Navigation*</u>

Different trajectories exploring the search space are shown in Fig. 15. The first trajectories begin at 26,000 ft. The maximal altitude where a flight can begin is at 40,000 ft and the maximal flight altitude is defined at 42,000 ft. The geodesic reference trajectory is at 36,000 ft (purple) and the global best is at 36,000 ft with a step climb of 2,000 ft at around 2000 nm (yellow).

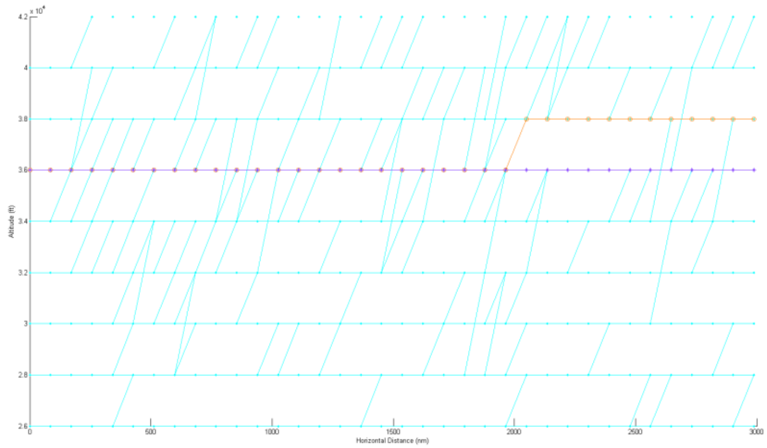

Fig. 15 Trajectories occupied all the search space in Vertical Navigation

Fig. 16 shows a cluster of trajectories at the next position *X* after the displacement *D*. It can be seen that trajectories came closer together towards the global and the local optimal (yellow and orange trajectories). Another evidence of this convergence is that there is not a single trajectory that begins at altitudes below 30,000 ft.

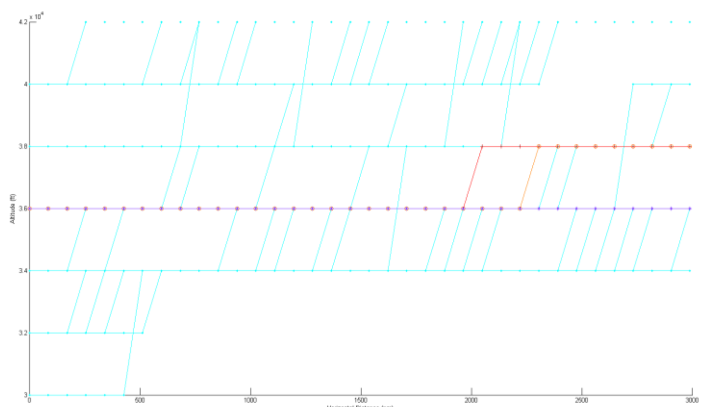

Fig. 16 Cluster of trajectories in Vertical navigation after the displacements

Fig. 17 shows all the local optima (and the global optimal) trajectories before the PSO is executed.

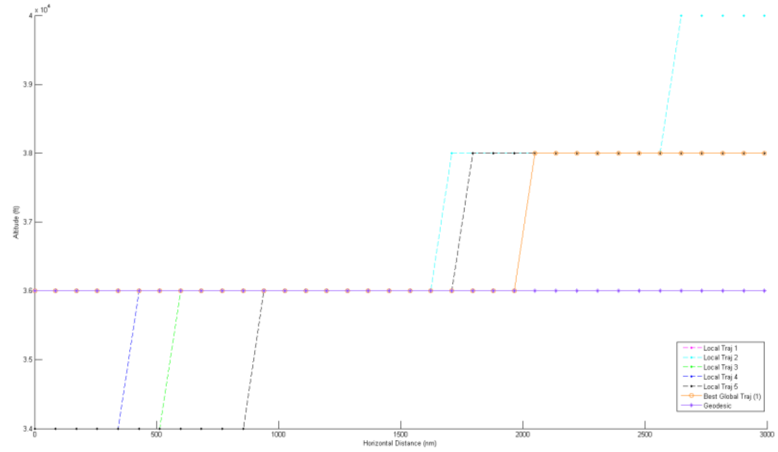

Fig. 17 Best local trajectories before the PSO

Fig 18 shows the local optima (and the global optimal) trajectories after the PSO is executed. Here it can be seen that most of the trajectories converge to the global optimal. It can also be seen that the global optimal began at 36,000 ft as in the beginning, but the PSO algorithm suggested moving the 2,000 ft step climb location from around 2,000 nm to around 2,250 nm. This was possible due to the search space exploration.

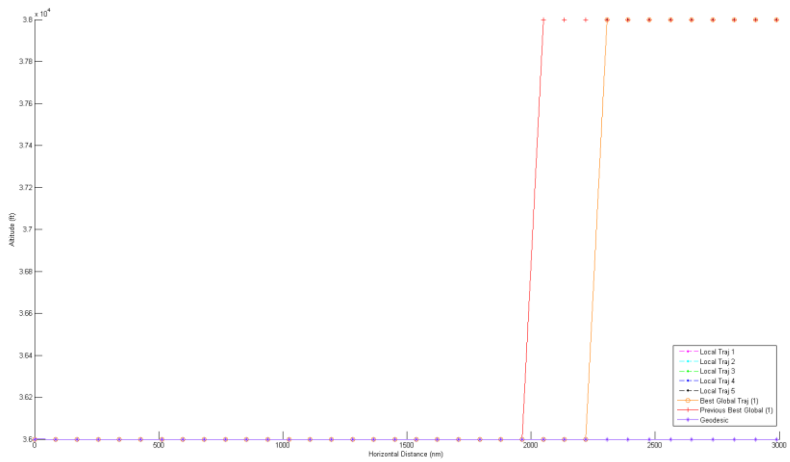

Fig 18 Evolution of the local trajectories after the PSO

Lateral Reference Trajectory

Fig. 19 represents all the initial trajectories in the lateral dimension. The geodesic is shown in purple, and the global best trajectory is shown in orange. All the trajectories are around the geodesic but as expected they present a random behavior.

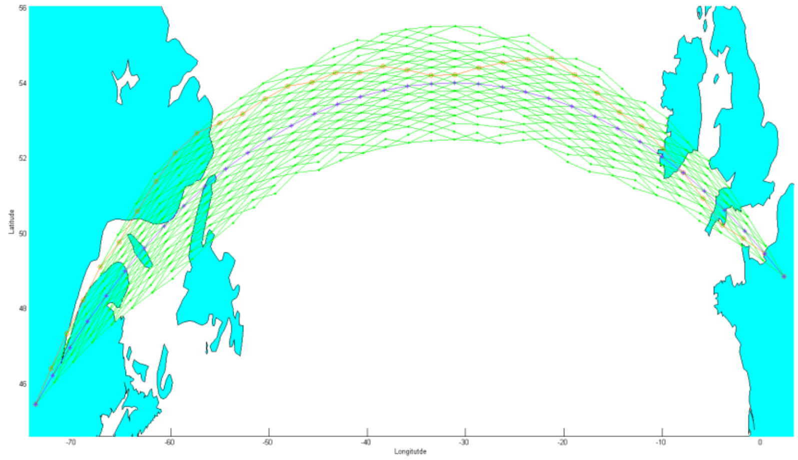

Fig. 19 Trajectories in Lateral Navigation before the PSO

Fig. 20 shows the updated trajectories position *X* after some displacements. It can be seen that many trajectories are coming closer to the global best. This is due to the convergence to the global optimal. It can also be seen that the global optimal changed. The previous global best trajectory is shown in red, the geodesic is again shown in purple, and the new global best trajectory is shown in orange.

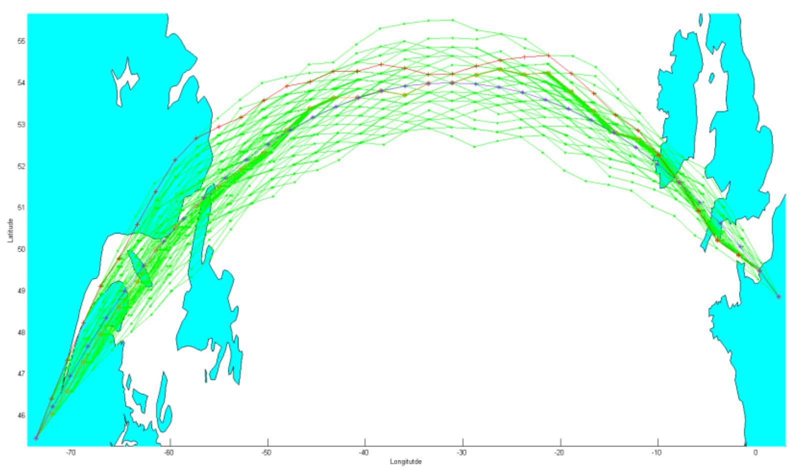

Fig. 20 Trajectories in Lateral Navigation after the PSO

Figure 21 and Fig 22 show the best global trajectories (local and optinal) before (Fig. 21) and after (Fig. 22) the PSO is executed. In these Figures, the global optimal influence in moving trajectories is evident.

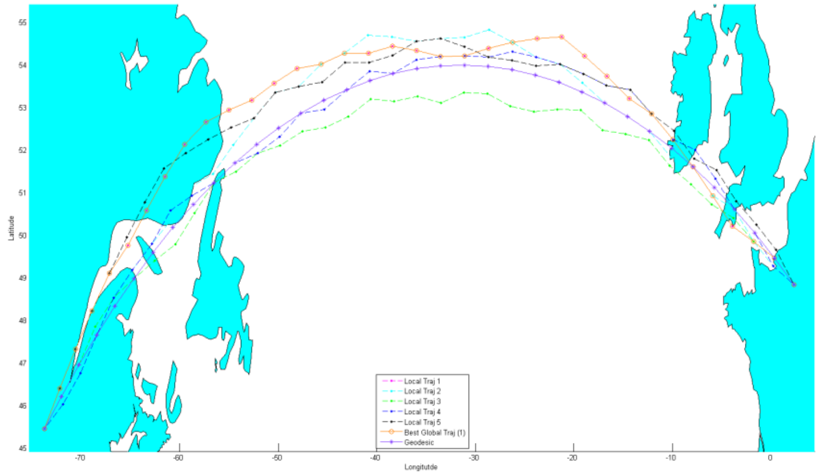

Fig. 21 Local trajectories before the PSO

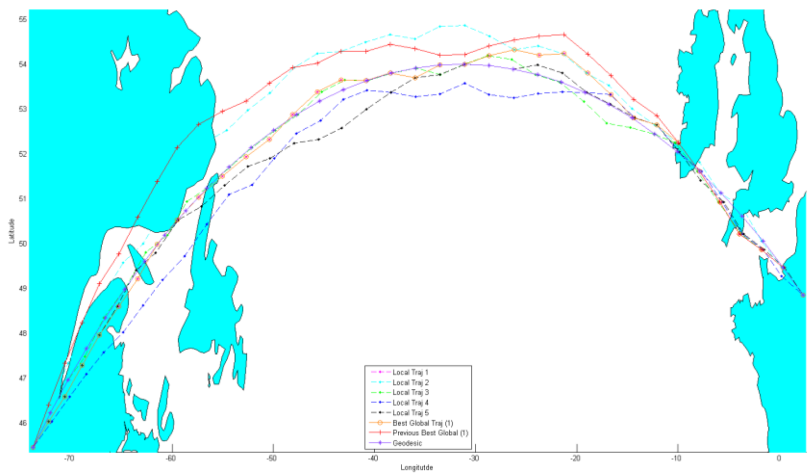

Fig. 22 Local trajectories after the PSO

Fig 22 also shows how the previous global optimal was influenced by the light blue local trajectory. The behaviour of the green, the black and the dark blue local trajectories tends to converge with the current global optimal.

2. Results with different flights

The flight cost of the trajectory provided by the PSO was compared against the flight cost of that trajectory following the geodesic at a fixed altitude of 34,000 ft following the great circle. The evaluated trajectories were Montreal (CDG) to Paris (CDG) with a distance of 2981nm, Toronto (YYZ) to London (LDH) with a distance of 3085 nm, Montreal to Vienna (VIE) with a distance of 3470 nm, and Vancouver (YVR) to Las Palmas (LPA) with a distance of 4658 nm.

Fig. 23 shows that the trajectories proposed by the algorithm reduced the fuel burn (thus emissions) during the flight and for this reason; the flight cost is reduced.

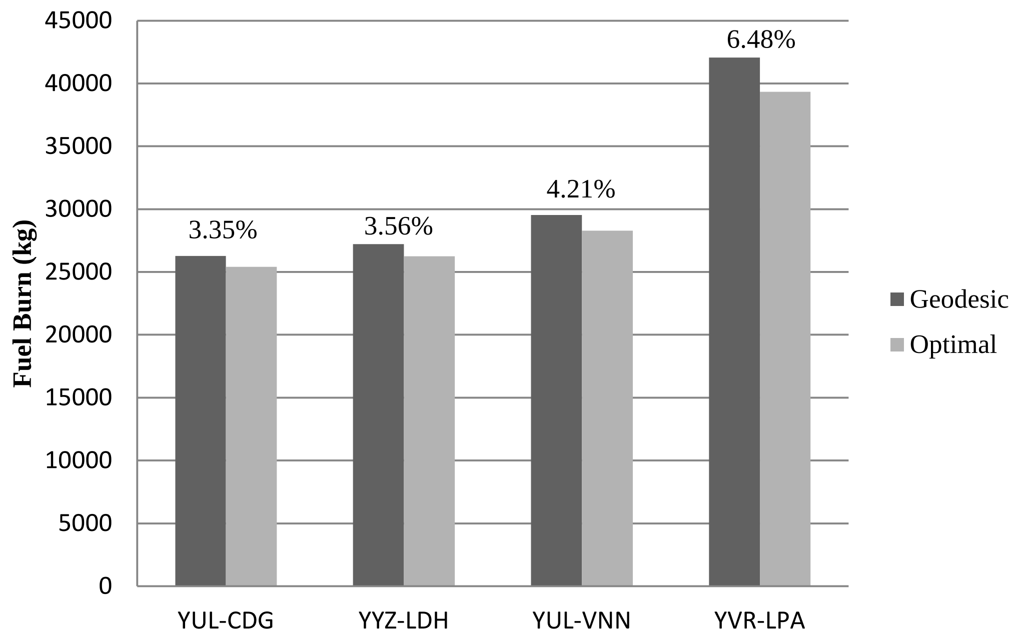

Fig. 23 Fuel burn saved between the geodesic trajectory and the optimal trajectory

As it can be seen the algorithm found better results the longer the trajectory, this is expected as more step climbs can be executed. This can also be explained as if the algorithm decides it to perform a step climb at a waypoint, it is so because it found better weather conditions and a more convenient altitude for the aircraft weight. If at this point there is a tailwind, the aircraft will reduce his consummation because it uses the force of the wind to fly at higher speeds than the ones provided by the thrust.

V. Conclusion

The PSO was able to provide trajectories able to reduce the flight cost while comparing against simple trajectories such as constant altitudes. As expected it was also observed that the longest the flight, the more optimization was obtained as the aircraft was able to find better wind currents and better pressure conditions.

However, it is of interest to compare the flight cost optimization against as flown trajectories in order to obtain more realistic results.

It was also observed that the optimized reference trajectories provide coherent results as the trajectories do not present consecutives changes of altitude or high variation in headwind for the lateral reference trajectory.

As future work, it is of interest to adjust the required time of arrival constraint to the algorithm in order to make them useful for the coming airspace regulations.

Acknowledgments

This Research was conducted in The Research Laboratory in Active Controls, Avionics and Aeroservoelasticity (LARCASE) for the global project "Optimized Descent and Cruise" with funds from the Business-led Network of Centers of Excellence Green Aviation Research & Development Network (GARDN). For more information please visit http://larcase.etsmtl.ca. The authors would like to thank Rex Haygate, Dominique Labour and Yvan Blondeau from CMC-Electronics – Esterline, and Oscar Carranza from LARCASE. The authors would like to thank CONACYT in Mexico and the FQRNT in Quebec, Canada.

References

[1.] Williams, P., D. . "Transatlantic flight times and climate change," *Environmental Research Letters* Vol. 11, No. 2, 2016, p. 024008. doi: http://dx.doi.org/10.1088/1748-9326/11/2/024008

[2.] ICAO. "Aviation's contribution to climate change." International Civil Aviation Organization, Montreal, 2010, p. 260

[3.] Freitag, W., Terry, Shulze E. "Blended Winglets Improve Performance," *Aeromagazine Boeing*, No. 35, 2009, pp. 9-12.

[4.]Gabor, O. Ș., Simon, A., Koreanschi, A., and Botez, R. M. "Improving the UAS-S4 Éhecal airfoil high angles-of-attack performance characteristics using a morphing wing approach," *Proceedings of the Institution of Mechanical Engineers, Part G: Journal of Aerospace Engineering* Vol. 230, No. 1, 2015, pp. 118-131. doi: 10.1177/0954410015587725
[5.]Randt, N. P., Jessberger, C., and Ploetner, K. O. "Estimating the Fuel Saving Potential of Commercial Aircraft in Future Fleet-Development Scenarios," *15th AIAA Aviation Technology, Integration, and Operations Conference*, 2015, Dallas, Texas, 2015,doi: http://dx.doi.org/10.2514/6.2015-2435
[6.]McConnachie, D., Wollersheim, C., and Hansman, R. J. "The Impact of Fuel Price on Airline Fuel Efficiency and Operations," *2013 Aviation Technology, Integration, and Operations Conference*. American Institute of Aeronautics and Astronautics, 2013.
[7.]Balakrishnan, H. "Control and optimization algorithms for air transportation systems," *Annual Reviews in Control* Vol. 41, 2016, pp. 39-46.doi: http://dx.doi.org/10.1016/j.arcontrol.2016.04.019
[8.]Jensen, L., Hansman, J. R., Venuti, J., and Reynolds, T. "Commercial Airline Altitude Optimization Strategies for Reduced Cruise Fuel Consumption," *14th AIAA Aviation Technology, Integration, and Operations Conference*. American Institute of Aeronautics and Astronautics, 2014.
[9.]Jensen, L., Hansman, J. R., Venuti, J. C., and Reynolds, T. "Commercial Airline Speed Optimization Strategies for Reduced Cruise Fuel Consumption," *2013 Aviation Technology, Integration, and Operations Conference*, 2013, Los Angeles, USA, 2013,doi: http://dx.doi.org/10.2514/6.2013-4289
[10.]Reynolds, T. G. "Green Aircraft Operations," *Encyclopedia of Aerospace Engineering*. John Wiley & Sons, Ltd, 2015, pp. 1-12.
[11.]Liden, S. "Optimum cruise profiles in the presence of winds," *Digital Avionics Systems Conference, 1992. Proceedings., IEEE/AIAA 11th*. Seattle, WA, 1992, pp. 254-261,doi: 10.1109/dasc.1992.282147
[12.]Dancila, B., Botez, R. M., and Labour, D. "Fuel Burn Prediction Algorithm for Cruise, Constant Speed and Level Flight Segments," *The Aeronatuical Journal* Vol. 117, No. 1191, 2013.
[13.]Sidibe, S., and Botez, R. M. "Trajectory optimization of FMS-CMA 9000 by dynamic programming," *ASI AÉRO 2013 conference, 60th Aeronautics Conference and AGM*, 2013, Toronto, Canada, 2013,doi:
[14.]Felix Patron, R. S., Botez, R. M., and Labour, D. "New Altitude Optimisation Algorithm for the Flight Management System CMA-9000 Improvement on the A310 and L-1011 Aircraft," *The Aeronautical Journal* Vol. 117, No. 1194, 2013, pp. 787-805.
[15.]Murrieta-Mendoza, A., Beuze, B., Ternisien, L., and Botez, R. "Branch & Bound-Based Algorithm for Aircraft VNAV Profile Reference Trajectory Optimization," *15th AIAA Aviation Technology, Integration, and Operations Conference, Aviation Forum*. AIAA, Dallas, TX, USA, 2015,doi: http://dx.doi.org/10.2514/6.2015-2280
[16.]Murrieta-Mendoza, A., and Botez, R. M. "Aircraft Vertical Route Optimization Deterministic Algorithm for a Flight Management System," *SAE 2015 AeroTech Congress & Exhibition*, 2015, Seattle, USA, 2015,doi: http://dx.doi.org/10.4271/2015-01-2541
[17.]Valenzuela, A., and Rivas, D. "Optimization of Aircraft Cruise Procedures Using Discrete Trajectory Patterns," *Journal of Aircraft* Vol. 51, No. 5, 2014, pp. 1632-1640. doi: http://dx.doi.org/10.2514/1.C032041
[18.]Rippel, E., Bar-Gill, A., and Shimkin, N. "Fast Graph-Search Algorithms for General-Aviation Flight Trajectory Generation," *Journal of Guidance, Control, and Dynamics* Vol. 28, No. 4, 2005, pp. 801-811. doi: http://dx.doi.org/10.2514/1.7370
[19.]Murrieta-Mendoza, A., and Botez, R. M. "Lateral Navigation Optimization Considering Winds And Temperatures For Fixed Altitude Cruise Using The Dijkstra's Algorithm," *International Mechanical Engineering Congress & Exposition*. Montreal, Canada, 2014,doi: http://dx.doi.org/10.1115/IMECE2014-37570
[20.]Ng, H. K., Sridhar, B., and Grabbe, S. "Optimizing Aircraft Trajectories with Multiple Cruise Altitudes in the Presence of Winds," *Journal of Aerospace Information Systems* Vol. 11, No. 1, 2014, pp. 35-47. doi: http://dx.doi.org/10.2514/1.I010084
[21.]Dicheva, S., and Bestaoui, Y. "Three-Dimensional A* Dynamic Mission Planning for an Airborne Launch Vehicle," *Journal of Aerospace Information Systems* Vol. 11, No. 2, 2014, pp. 98-106. doi: http://dx.doi.org/10.2514/1.I010070
[22.]Félix-Patrón, R. S., Berrou, Y., and Botez, R. M. "New Methods of Optimization of the Flight Profiles for Performance Database-Modeled Aircraft," *Proceedings of the Institution of Mechanical Engineers, Part G: Journal of Aerospace Engineering*, 2014. doi: 10.1177/0954410014561772
[23.]Soler, M., Zou, B., and Hansen, M. "Flight trajectory design in the presence of contrails: Application of a multiphase mixed-integer optimal control approach," *Transportation Research Part C: Emerging Technologies* Vol. 48, 2014, pp. 172-194. doi: http://dx.doi.org/10.1016/j.trc.2014.08.009
[24.]Sridhar, B., Ng, H., and Chen, N. "Aircraft Trajectory Optimization and Contrails Avoidance in the Presence of Winds," *Journal of Guidance, Control, and Dynamics* Vol. 34, No. 5, 2013, pp. 1577-1584. doi: 10.2514/1.53378
[25.]Hagelauer, P., and Mora-Camino, F. "A Soft Dynamic Programming Approach for On-Line Aircraft 4D-Trajectory Optimization," *European Journal of Operational Research* Vol. 107, No. 1, 1998, pp. 87-95. doi: http://dx.doi.org/10.1016/S0377-2217(97)00221-X
[26.]Miyazawa, Y., Wickramasinghe, N. K., Harada, A., and Miyamoto, Y. "Dynamic Programming Application to Airliner Four Dimensional Optimal Flight Trajectory," *AIAA Guidance, Navigation, and Control (GNC) Conference*. American Institute of Aeronautics and Astronautics, Boston, USA, 2013,doi: http://dx.doi.org/10.2514/6.2013-4969

[27.]Félix-Patrón, R. S., and Botez, R. M. "Flight Trajectory Optimization Through Genetic Algorithms for Lateral and Vertical Integrated Navigation," *Journal of Aerospace Information Systems* Vol. 12, No. 8, 2015, pp. 533-544. doi: http://dx.doi.org/10.2514/1.I010348

[28.]Murrieta-Mendoza, A., Bunel, A., and Botez, R. M. "Aircraft Vertical Reference Trajectory Optimization With a RTA Constraint Using the ABC Algorithm," *16th AIAA Aviation Technology, Integration, and Operations Conference*. American Institute of Aeronautics and Astronautics, Washington, D.C., 2016,doi: http://dx.doi.org/10.2514/6.2016-4208

[29.]Murrieta-Mendoza, A., Hamy, A., and Botez, R. M. "Lateral Reference Trajectory Algorithm Using Ant Colony Optimization," *16th AIAA Aviation Technology, Integration, and Operations Conference*. American Institute of Aeronautics and Astronautics, Washington, D.C., 2016,doi: http://dx.doi.org/10.2514/6.2016-4209

[30.]Murrieta-Mendoza, A., Hamy, A., and Botez, R. M. "Mach Number Selection for Cruise Phase using the Ant Colony Optimization Algorithm With RTA Constrains," *International Conference on Air Transport*. Amsterdam, Netherlands, 2015,

[31.]Ojha, S. K. "Optimization of Cruising Flights of Turbojet Aircraft," *Flight Performance of Aircraft*. American Institute of Aeronautics and Astronautics, 1995, pp. 237-258.